A Partial Variational Approach for Arbitrary Discontinuities in Planar Dielectric Waveguides

SHYH-JONG CHUNG AND CHUN HSIUNG CHEN

Abstract—A novel approach for analyzing arbitrary discontinuities in planar dielectric waveguides is proposed that uses the finite-element method along with the frontal solution technique. Based on the partial variational principle (PVP), the fields interior and exterior to the discontinuity finite element region can be treated independently and eventually can be coupled. The interior fields are expanded by the finite element nodal values and the corresponding local bases, while the exterior ones are handled by an approach combining modal expansion and Green's function. In numerical computation, the continuous spectra of the waveguide modes are discretized by the Laguerre expansion method.

To check the correctness of the present analysis, two numerical results are compared with those of other methods. The scattering characteristics of several linearly tapered discontinuities, such as transformers and feed structures, are analyzed and compared with those having step junctions.

I. Introduction

PLANAR dielectric waveguides are important in millimeter-wave, submillimeter-wave, and optical systems. Discontinuities are often introduced to create such components as transformers, grating couplers, and feed structures. They also occur as a consequence of the misalignment in component interconnections. Thus, many authors have paid attention to the discontinuity problems associated with planar dielectric waveguides [1]–[17].

Analysis of associated discontinuity problems is difficult owing to the excitation of guided modes and radiation modes which have a continuous spectrum. Several techniques have been proposed to deal with the continuous spectrum in actual numerical computation [3]–[13]. Mahmoud and Beal [5] used the normalized Laguerre polynomials to expand the continuous spectrum, and then applied the mode-matching method to solve a step discontinuity problem. Rozzi [6] instead applied the same polynomials to express the tangential fields at the junction of a step discontinuity and proposed the Ritz–Galerkin variational approach for solution.

These methods are effective only if the discontinuities are of the abrupt step type. But the analysis of arbitrary discontinuities is also necessary from practical considerations. For small, smoothly varying discontinuities, Marcuse [14] solved a tapered dielectric slab waveguide by regarding the structure as a succession of an infinite number of infinitesimal steps. Miyanaga and Asakura [15] used the perturbation theory to study a linearly tapered grating coupler.

For arbitrarily varying discontinuities, the finite element approach has been adopted to expand the field distribution in the discontinuity region [16], [17]. In this approach, treatment of the fields exterior to the finite element (discontinuity) region poses a considerable challenge. Suzuki and Koshiba [16] put a semi-infinite electric conductor far above the discontinuities and used the Green's functions of the waveguides to obtain a representation of the boundary fields. Recently, Chung and Chen [17] treated the problem of arbitrary irregularities in an otherwise uniform slab waveguide by using the Green's function of the waveguide to express the exterior fields in terms of the fields in the irregularity region. However, this approach seems useless when the two slab guides connected to the discontinuity are different, because of the difficulty in finding the Green's function.

In this investigation, the problem with completely arbitrary discontinuities in different dielectric slab waveguides will be attacked. The fields interior and exterior to the discontinuity finite element region will be properly handled and coupled based on the partial variational principle (PVP) [18] and the finite element method. Several linearly tapered discontinuities will then be investigated in detail with numerical results to show the scattering characteristics of the structures.

II. Formulation of the Problem

Consider the planar dielectric waveguide structure with discontinuity shown in Fig. 1(a), which is uniform in the y direction and symmetric with respect to the $y-z$ plane. Suppose that symmetric guided TE modes with y-polarized electric fields are incident from $z=-\infty$ and $z=+\infty$. Basically, we may consider the reduced structure shown in Fig. 1(b), where a discontinuity region Ω with refractive index $n(x,z)$ is enclosed by three artificial boundaries $\Gamma_1, \Gamma_2, \Gamma_3$, and a magnetic wall Γ_0, which is introduced due to symmetry. Placed in region I $(0 \leqslant x < \infty, z \leqslant 0)$ and region II $(0 \leqslant x < \infty, z \geqslant l)$ are planar dielectric wave-

Manuscript received March 9, 1988; revised June 13, 1988. This work was supported by the National Science Council, Republic of China, under Grant NSC 77-0404-E002-01.

The authors are with the Department of Electrical Engineering, National Taiwan University, Taipei, Taiwan, Republic of China.

IEEE Log Number 8824240.

0018-9480/89/0100-0208$01.00 ©1989 IEEE

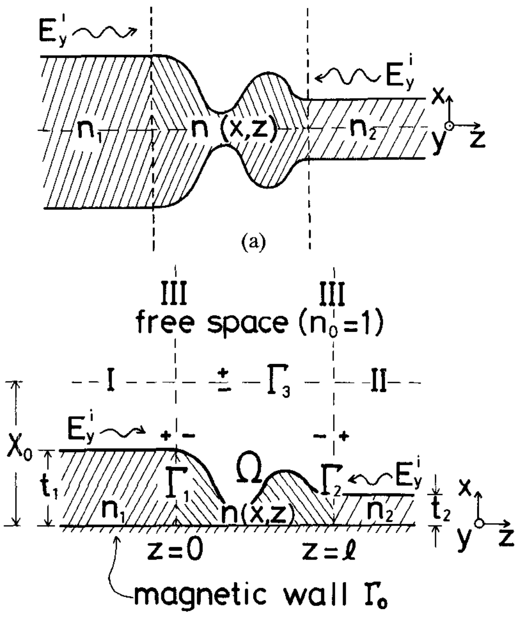

Fig. 1. (a) Original structure with arbitrary discontinuity in planar dielectric waveguide. (b) Reduced structure for solution.

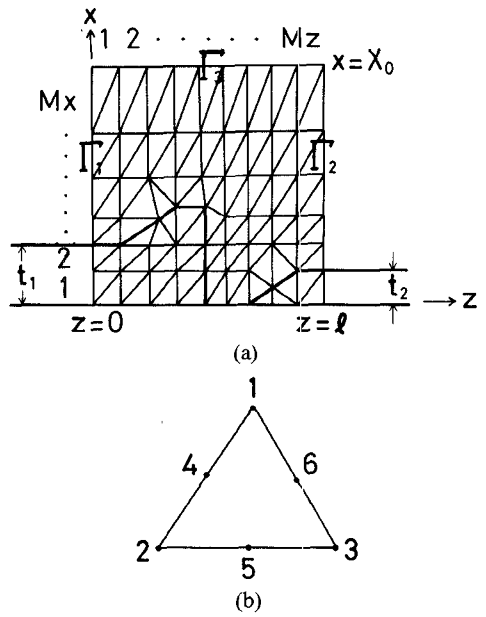

Fig. 2. (a) Typical mesh division for linearly tapered discontinuity in planar dielectric waveguide ($M_x \times M_z = 6 \times 9$). (b) Second-order triangular element.

guides I and II, respectively, whose refractive indices are n_1 and n_2. Region III is free space, which is above the artificial boundary $x = X_0$. Note the overlapping of regions I and III as well as II and III.

From the partial variational principle, a variational equation is obtained [18], [17]:

$$\delta^a I^a = 0$$

$$I^a = \frac{j}{\omega\mu_0}\int_\Omega dv\left[\frac{\partial E_y^a}{\partial x}\frac{\partial E_y}{\partial x} + \frac{\partial E_y^a}{\partial z}\frac{\partial E_y}{\partial z} - k_0^2 n^2 E_y^a E_y\right] + \int_\Gamma ds\,\hat{n}\cdot\left[\hat{z}H_x^a(\Gamma^+) - \hat{x}H_z^a(\Gamma^+)\right]\cdot\left[E_y(\Gamma^-) - E_y(\Gamma^+)\right] - \int_\Gamma ds\,E_y^a(\Gamma^-)\hat{n}\cdot\left[\hat{x}H_z(\Gamma^+) - \hat{z}H_x(\Gamma^+)\right] \quad (1)$$

where $\Gamma = \Gamma_1 + \Gamma_2 + \Gamma_3$ and $\hat{n}$ is its outward normal. Γ^- and Γ^+ represent the inner and outer sides of Γ, respectively. As usual, $k_0^2 = \omega^2\mu_0\epsilon_0$ and $n^2(x,z) = \epsilon(x,z)/\epsilon_0$, where $\epsilon(x,z)$ is the permittivity of the discontinuity region Ω. (E_y, H_x, H_z) are the undetermined trial fields, while (E_y^a, H_x^a, H_z^a) are test fields, which may be regarded as a set of weighting functions.

In applying (1), two points must be mentioned. The partial variational operator δ^a must operate only on the test fields with superscript a. The trial fields exterior to boundary Γ must obey the source-free and radiation conditions.

The fields in (1) may be classified into two groups: those interior and those exterior to the boundary Γ. Since the variational equation (1) actually contains the natural continuity boundary condition [18], these two groups of fields can first be treated independently and then be coupled in the process of solving the variational equation (1). The interior fields are tackled by the finite element method, which will be described in the next section. The exterior fields are further divided into two linked types: those in the waveguides and those in free space, which will be depicted in Sections IV and V.

III. Fields in the Discontinuity Region

The fields in the discontinuity region Ω are handled by the finite element method [19], [20]. To this end, the discontinuity region is divided into several elements, each with triangular shape, as shown in Fig. 2(a). For each element e, six nodes are specified (Fig. 2(b)) and the field E_y^e in that element is expanded by the nodal values ϕ_i^e and their corresponding shape functions N_i:

$$E_y^e(x,z) = \sum_{i=1}^{6}\phi_i^e N_i \quad (2)$$

where

$$N_1 = l_1(2l_1 - 1) \qquad N_2 = l_2(2l_2 - 1)$$
$$N_3 = l_3(2l_3 - 1) \qquad N_4 = 4l_1l_2 \quad (3)$$
$$N_5 = 4l_2l_3 \qquad N_6 = 4l_3l_1$$

and l_1, l_2, l_3 are the area coordinates [19]. The relation between the area coordinates and the Cartesian coordinates is given by

$$\begin{bmatrix} z \\ x \\ 1 \end{bmatrix} = \begin{bmatrix} z_1 & z_2 & z_3 \\ x_1 & x_2 & x_3 \\ 1 & 1 & 1 \end{bmatrix}\begin{bmatrix} l_1 \\ l_2 \\ l_3 \end{bmatrix} \quad (4)$$

where (x_j, z_j) are the Cartesian coordinates of the vertex j $(j = 1,2,3)$ of the triangle.

The fields in the whole discontinuity region are just the sum of those in each element:

$$E_y(\Omega)=\sum_e\sum_{i=1}^{6}\phi_i^e N_i \tag{5a}$$

$$\frac{\partial}{\partial\xi}E_y(\Omega)=\sum_e\sum_{i=1}^{6}\phi_i^e\frac{\partial}{\partial\xi}N_i, \qquad \xi=x,z. \tag{5b}$$

IV. Fields in Waveguide Regions

The fields in waveguides I and II are expressed as the combination of the waveguide modes:

$$E_y^\alpha(x,z)=\sum_{p=1}^{N_\alpha}\left[A_p^\alpha e^{\mp j\beta_p^\alpha(z-z_\alpha)}+a_p^\alpha e^{\pm j\beta_p^\alpha(z-z_\alpha)}\right]u_p^\alpha(x)+\int_0^\infty d\rho\, d_\rho^\alpha\frac{\omega\mu_0}{\beta_\rho}u_\rho^\alpha(x)e^{\pm j\beta_\rho^\alpha(z-z_\alpha)} \tag{6a}$$

$$\omega\mu_0 H_x^\alpha(x,z)=\mp\sum_{p=1}^{N_\alpha}\beta_p^\alpha\left[A_p^\alpha e^{\mp j\beta_p^\alpha(z-z_\alpha)}-a_p^\alpha e^{\pm j\beta_p^\alpha(z-z_\alpha)}\right]u_p^\alpha(x)\pm\omega\mu_0\int_0^\infty d\rho\, d_\rho^\alpha\, u_\rho^\alpha(x)e^{\pm j\beta_\rho(z-z_\alpha)} \tag{6b}$$

where $\alpha=$ I or II. When $\alpha=$ I, the upper signs are used; otherwise the lower ones are used. A_p and a_p are the coefficients of the incident (known) and scattered (unknown) pth guided modes, whose modal function and propagation constant are $u_p(x)$ and β_p. The quantities $u_\rho(x)$ and d_ρ are the modal function and the coefficient of the radiation mode, with ρ and $\beta_\rho=\sqrt{k_0^2-\rho^2}$ being the wavenumbers (continuous spectrum) in the x and z directions, respectively. N_α is the total number of guided modes in region α; and $z_\alpha=0$ or l, when $\alpha=$ I or II, respectively.

The scattering coefficients can be represented as a function of the magnetic fields at $z=z_\alpha$. Multiplying (6b) in turn by u_p^α and u_ρ^α, integrating over x at $z=z_\alpha$, and using mode orthogonality property, one obtains

$$a_p^\alpha=A_p^\alpha\pm\frac{1}{\beta_p^\alpha}\int_0^\infty dx\, u_p^\alpha(x)\,\omega\mu_0 H_x^\alpha(x,z_\alpha) \tag{7a}$$

$$d_\rho^\alpha=\pm\frac{1}{\omega\mu_0}\int_0^\infty dx\, u_\rho^\alpha(x)\,\omega\mu_0 H_x^\alpha(x,z_\alpha). \tag{7b}$$

Introduce a complete set in $0\leqslant x<\infty$ [6]:

$$\mathscr{L}_q(x)=\frac{1}{\sqrt{S_0}}\exp(-x/2S_0)L_{q-1}\left(\frac{x}{S_0}\right), \qquad q=1,2,\cdots \tag{8}$$

where L denotes the Laguerre polynomial. Deciding on the scale factor S_0 is quite complicated. Roughly speaking, it is chosen such that (9a) can essentially be satisfied for a given M [6]. (Actually, there exists a large range of S_0 which may satisfy the above requirement.) Besides, the sequence of (8) should be independent in $0\leqslant x\leqslant X_0$ and should be able to represent the field behavior in $0\leqslant x\leqslant X_0$. To be independent, S_0 may be chosen as small as possible. But when S_0 is too small, the Laguerre polynomials will vary quickly near $x=0$ and will be almost zero about $x=X_0$, which makes it difficult for the sequence of (8) to express the actual field behavior in the vicinity of $x=X_0$.

In terms of these normalized Laguerre polynomials, the modal functions of the waveguides can be expressed as

$$u_p^\alpha(x)=\sum_{q=1}^{M}Q_{pq}^\alpha\mathscr{L}_q(x) \tag{9a}$$

$$u_\rho^\alpha(x)=\sum_{q=1}^{M}P_{\rho q}^\alpha\mathscr{L}_q(x) \tag{9b}$$

where

$$Q_{pq}^\alpha=\int_0^\infty dx\, u_p^\alpha(x)\mathscr{L}_q(x) \tag{10a}$$

$$P_{\rho q}^\alpha=\int_0^\infty dx\, u_\rho^\alpha(x)\mathscr{L}_q(x) \tag{10b}$$

and M is a finite number in actual numerical computation.

Now let us expand the magnetic fields $\omega\mu_0 H_x$ as a sum of the incident fields and the combination of the normalized Laguerre polynomials:

$$\omega\mu_0 H_x(\Gamma_\alpha^+)=\omega\mu_0 H_x^\alpha(x,z_\alpha)=\mp\sum_{p=1}^{N_\alpha}\beta_p^\alpha A_p^\alpha u_p^\alpha(x)+\sum_{q=1}^{M}h_q^\alpha\mathscr{L}_q(x) \tag{11}$$

where the h_q's are to be determined.

With (11), (9a), and (9b), the scattering coefficients of (7a) and (7b) may be rewritten as

$$a_p^\alpha=\pm\sum_{q=1}^{M}h_q^\alpha\left(\frac{Q_{pq}^\alpha}{\beta_p^\alpha}\right) \tag{12a}$$

$$d_\rho^\alpha=\pm\sum_{q=1}^{M}h_q^\alpha\left(\frac{P_{\rho q}^\alpha}{\omega\mu_0}\right). \tag{12b}$$

Substituting (12a), (12b), (9a), and (9b) into (6a), one gets

$$E_y(\Gamma_\alpha^+)=E_y^\alpha(x,z_\alpha)=\sum_{p=1}^{N_\alpha}A_p^\alpha u_p^\alpha(x)\pm\sum_{q=1}^{M}h_q^\alpha\left[\sum_{t=1}^{M}Z_{qt}^\alpha\mathscr{L}_t(x)\right] \tag{13}$$

where

$$Z_{qt}^\alpha=\sum_{p=1}^{N_\alpha}\frac{1}{\beta_p^\alpha}Q_{pq}^\alpha Q_{pt}^\alpha+\int_0^\infty d\rho\frac{P_{\rho q}^\alpha P_{\rho t}^\alpha}{\beta_\rho}. \tag{14}$$

Equations (11) and (13) then give the tangential fields over the boundaries Γ_1 and Γ_2.

V. Fields in Free Space

The fields above the boundary $x = X_0$ may be represented by those over the boundary, using the Green's function in free space (see the Appendix):

$$E_y(x,z) = -\int_{-\infty}^{\infty} dz' G(x - X_0, z - z') \frac{\partial}{\partial x'} E_y(X_0, z'), \quad (x,z) \in \text{III} \quad (15a)$$

$$\begin{aligned} \omega\mu_0 H_z(x,z) &= -\int_{-\infty}^{\infty} dz' G(x - X_0, z - z') \frac{\partial}{\partial x'} \omega\mu_0 H_z(X_0, z') \\ &= -j\int_{-\infty}^{\infty} dz' G(x - X_0, z - z') \frac{\partial^2}{\partial x'^2} E_y(X_0, z'), \end{aligned} \quad (x,z) \in \text{III} \quad (15b)$$

where the Green's function G takes the form

$$G(x - x', z - z') = -\frac{j}{2} H_0^{(2)}\left(k_0\sqrt{(x - x')^2 + (z - z')^2}\right). \quad (16)$$

The integrations in (15a) and (15b) can be divided into three parts, that is, $-\infty < z' \leqslant 0$, $l \leqslant z' < \infty$, and $0 \leqslant z' \leqslant l$. The fields in first two parts are calculated by partially differentiating (6a) with respect to x, and thus are functions of A_p^α and h_q^α as a result of (12a) and (12b). For the last part, i.e., the integration along $0 \leqslant z' \leqslant l$, the field in (5b) is substituted into (15a). To avoid double differentiation with respect to the local second-order bases N_t, the source term in (15b) need special treatment. From the Helmholtz equation, one has

$$\frac{\partial^2 E_y}{\partial x'^2} = -k_0^2 E_y - \frac{\partial^2 E_y}{\partial z'^2}. \quad (17)$$

By using (17) and integration by parts, the integral (15b) in $0 \leqslant z' \leqslant l$, denoted by $\omega\mu_0 H_{z3}$, becomes

$$\begin{aligned} \omega\mu_0 H_{z3}(x,z) &= -j\int_0^l dz' G(x - X_0, z - z') \frac{\partial^2}{\partial x'^2} E_y(X_0, z') \\ &= jk_0^2 \int_0^l dz' G(x - X_0, z - z') E_y(X_0, z') \\ &\quad + jG(x - X_0, z - z') \frac{\partial}{\partial z'} E_y(X_0, z') \Big|_{z'=0}^{l} \\ &\quad - j\int_0^l dz' \frac{\partial}{\partial z'} G(x - X_0, z - z') \frac{\partial}{\partial z'} E_y(X_0, z'). \end{aligned} \quad (18)$$

Note that we have reduced the order of differentiation to just one.

From the preceding derivation, it is concluded that the fields in region III, (15a) and (15b), are now functions of A_p^α, h_p^α, and the nodal values ϕ_t of the elements adjacent to Γ_3:

$$E_y(\Gamma_3^+) = \sum_\alpha \left[\sum_p E_p^\alpha A_p^\alpha + \sum_q E_q^\alpha h_q^\alpha\right] + \sum_t E_t \phi_t \quad (19a)$$

$$\omega\mu_0 H_z(\Gamma_3^+) = \sum_\alpha \left[\sum_p H_p^\alpha A_p^\alpha + \sum_q H_q^\alpha h_q^\alpha\right] + \sum_t H_t \phi_t \quad (19b)$$

where the E's and H's are known functions of X_0 and z.

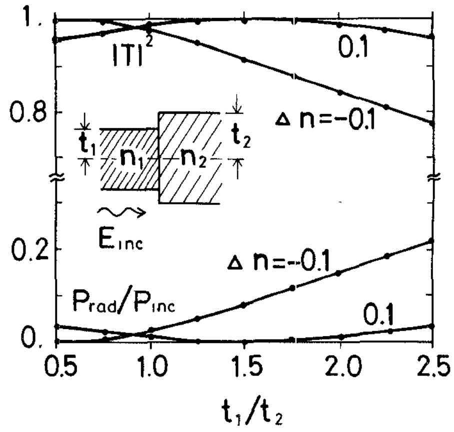

Fig. 3. Normalized transmitted power $|T|^2$ and radiation loss $P_{\text{rad}}/P_{\text{inc}}$ of step discontinuity. $k_0 t_1 = 0.55$, $n_1 = 1.6$, $n_2 = n_1(1 + \Delta n)$. — present analysis ($M = 7$); $\cdots\cdot$ Hosono *et al.* [9].

VI. Numerical Results

By using the Ritz–Galerkin approach [19], the variational equation (1) is solved by the finite element method and the frontal solution technique [20], using the exterior fields (11), (13), (19a), and (19b). After the assembly and elimination processes of the frontal solution technique, we finally get a matrix equation of the form

$$\bar{\bar{A}} \cdot \bar{\varphi} = \bar{s} \quad (20)$$

where $\bar{\bar{A}}$ is a known matrix, while $\bar{\varphi}$ and $\bar{s}$ are vectors associated with the unknown coefficients and the source terms due to the incident fields, respectively. Specifically $\bar{\varphi} = [\phi_t, h_q^{\text{I}}, h_q^{\text{II}}]^T$, where ϕ_t are the nodal values along the boundaries Γ_1, Γ_2, and those of the elements adjacent to Γ_3. After the unknowns h_q^α's are solved, (12a) and (12b) can then be used to obtain the scattering coefficients of the waveguide modes.

For an accuracy check, two well-known examples are again studied and compared with those solved by other methods. Here the reflection coefficient R and the transmission coefficient T are, respectively, equal to a_1^{I} and a_1^{II} of (6a) with A_p^{II} equal to 0, and the normalized radiated power $P_{\text{rad}}/P_{\text{inc}} = 1 - |R|^2 - |T|^2$. Fig. 3 shows the normalized transmitted power ($= |T|^2$) and radiated power of a step discontinuity, with the ratio t_1/t_2 of the waveguide widths a variable and the normalized difference Δn of the refractive indices a parameter. Our results show excellent agreement with those of Hosono *et al.* [9]. Fig. 4 also shows good agreement between the present results and those of Chung and Chen [17] for the discontinuity shown in the figure. The length of the discontinuity is fixed, while its height h is changed. The special case $h/D = -1$ corresponds to one of an air gap.

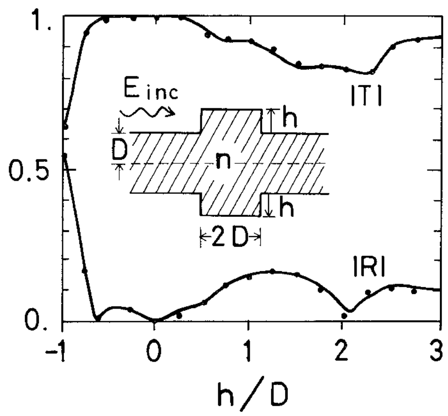

Fig. 4. Reflection and transmission coefficients of rectangular discontinuity. $K_0D = 1$, $n = 2.236$. — present analysis ($M_x \times M_z = 8\times5$, $X_0/D = 6$, $M = 7$); $\cdots\cdot$ Chung and Chen [17].

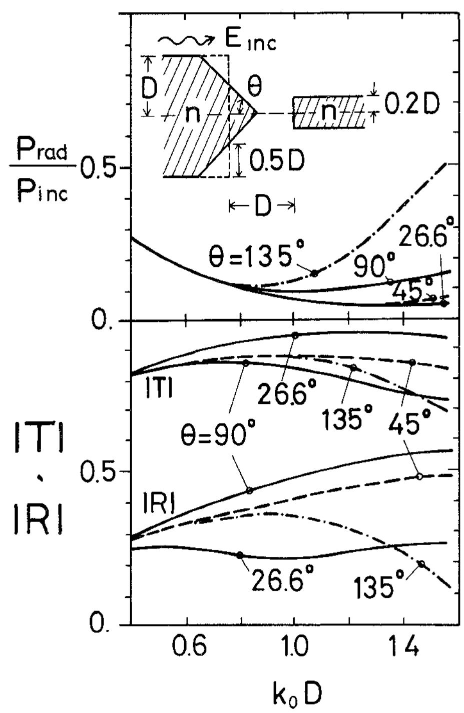

Fig. 5. Reflection coefficients, transmission coefficients, and radiation losses of feed structure. $n = 2.236$, $M = 7$.

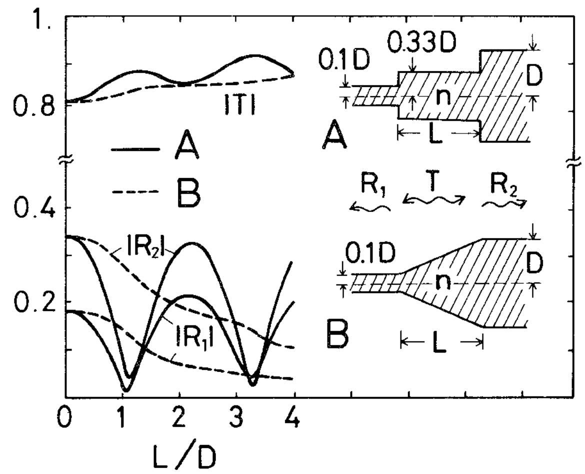

Fig. 6. Reflection and transmission coefficients of two ten-to-one transformers. $k_0D = 1$, $n = 2.236$, $M_x = 14$, $M = 7$, $X_0/D = 6$.

In Fig. 5 we consider a possible feed structure which has a discontinuity governed by the half angle of the tip θ. Shown here are the reflection coefficient $|R|$, the transmission coefficient $|T|$, and the normalized radiated power $P_{\text{rad}}/P_{\text{inc}}$ as a function of the normalized frequency k_0D. For $\theta = 90°$, the feed end is a step one, and for θ greater or smaller than 90°, the end is concave or convex, respectively. When $\theta = 26.6°$, the tip of the feed end just touches the right waveguide. The three sets of curves are independent of θ when k_0D approaches 0, due to the smallness of the discontinuity region. When $k_0D \geqslant 1$, the radiation losses for the concave case ($\theta = 135°$) are relatively large compared with those of other cases. It is seen that although the radiation losses for $\theta = 26.6°$ and 45° are nearly the same for all k_0D, the former has higher transmission as well as lower reflection coefficients, which means that a better feed condition can be reached.

The characteristics of two ten-to-one transformers, one with abrupt steps (structure A) and the other with a linear taper (structure B), are compared in Fig. 6. For the given values of the parameters, both left and right waveguides are monomode. For structure A, the width of the midsection is chosen so that the impedance-matching conditions are satisfied. The fields scattered by the step junctions (structure A) interfere with each other; thus two dips in the curves of the reflection coefficients are observed. Without strong reflection in structure B, the corresponding curves for the tapered structure behave more smoothly than those in the step one. The CPU time is quite different when the normalized length L/D of the taper is changed. For example, about 2 minutes are required for calculating the scattering coefficients of structure A for $L/D = 0$, with the division $M_x \times M_z = 14\times2$ (Fig. 2(a)), while 5 minutes are required for $L/D = 2$ ($M_x \times M_z = 14\times7$), both with a DEC VAX 11/780.

To discuss the frequency response of the ten-to-one transformers, we study the adjustable tapered transformer structure shown in the insert of Fig. 7. The length of the transformer is constant ($=1.1\ D$) with respect to the widths of the waveguides. When the tilt angle θ equals 0°, the width of the midsection is 0.33 D, like that of structure A (Fig. 6). When θ is different from 0°, the structure is so determined that the two step ratios, namely th ratio of the waveguide widths immediately adjacent to the junction, are approximately the same. Specifically the structure with $\theta = 39.3°$ corresponds to structure B of Fig. 6, where the step ratios are equal to 1. It is noticed that the length of the midsection is chosen to correspond to the first dip of $|R_1|$ in Fig. 6 (where $k_0D = 1$). The subscript 1 (2) in R and P_{rad} denotes the ones with wave incident from waveguide I (II). By reciprocity, $T_1 = T_2 = T$. From the reflection curves, it is seen that the bandwidth of $\theta° = -20$ is nearly equal to that of $\theta = 0°$, but with the minimum shifting toward the lower frequency. Here the bandwidth means the width of the normalized frequency for a given

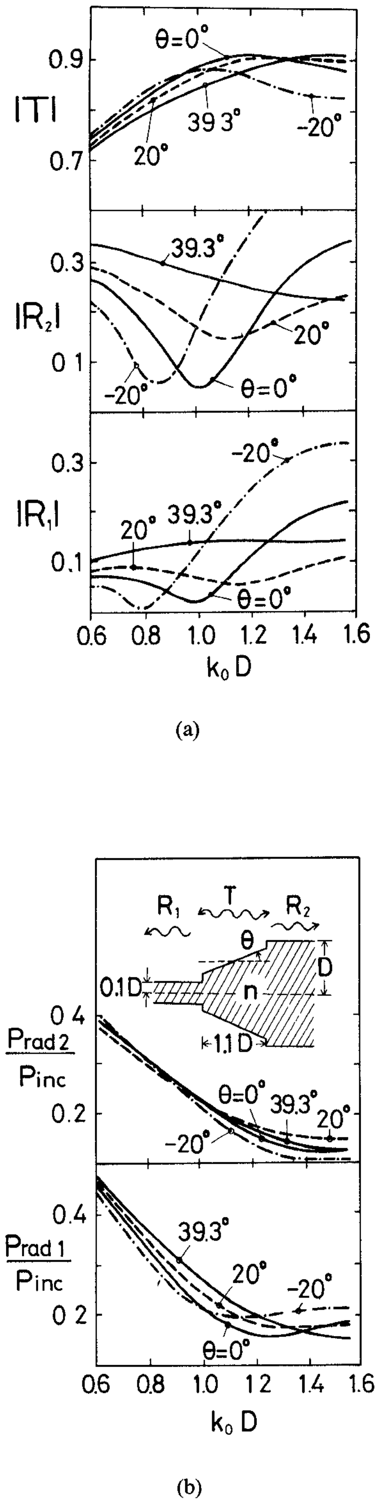

Fig. 7. (a) Reflection and transmission coefficients. (b) Normalized radiation losses of a ten-to-one adjustable tapered transformer. $n = 2.236$, $M = 7$.

level of reflection coefficient. As θ increases, the bandwidth broadens and the minimum becomes larger and shifts toward the higher frequency. Note that as $k_0 D \leqslant 1$, the radiation losses increase as $k_0 D$ decreases, which means that the radiation loss at the minimum of $\theta = -20°$ is larger than that of $\theta = 0°$, although their reflection minima are approximately the same.

VII. Conclusions

Based on the partial variational principle and the finite element method, we have proposed a method for analyzing the slab discontinuity problems that do not fall into the abrupt step category. Two types of exterior fields have been linked to represent the whole exterior fields. By comparing the numerical results for step discontinuities with those from other methods, we have checked the accuracy of the present approach. In this investigation, several components having tapered structures have been examined. In general, the tapered structure may reduce the radiation loss and/or increase the bandwidth of the components. With this method, more complicated discontinuity problems with TE- or TM-mode incidence can also be solved.

Appendix
Field Representation in (15a) and (15b)

Let G be the two-dimensional Green's function in free space and ϕ the scalar wave function ($\phi = E_y$ or $\omega\mu_0 H_z$) such that

$$\nabla_t^2 G + k_0^2 G = -\delta(x - x', z - z') \qquad \text{(A1)}$$

and

$$\nabla_t^2 \phi + k_0^2 \phi = 0 \qquad \text{(A2)}$$

where ∇_t^2 denotes the two-dimensional Laplacian operator. Multiplying (A1) by ϕ and (A2) by G, subtracting the result of the former from that of the latter, and then integrating over the half space $x \geqslant X_0$, $-\infty < x < \infty$, one obtains

$$\phi(x', z') = \int_{x \geqslant X_0} dx\,dz \left(G\nabla_t^2\phi - \phi\nabla_t^2 G\right) = -\int_{-\infty}^{\infty} dz \left(G\frac{\partial\phi}{\partial x} - \phi\frac{\partial G}{\partial x}\right)\Bigg|_{x = X_0}. \qquad \text{(A3)}$$

Here the two-dimensional Green's theorem and the radiation condition have been used.

Choose G as

$$G(x, z; x', z') = -\frac{j}{4}\left[H_0^{(2)}(k_0 r) + H_0^{(2)}(k_0 r_1)\right] \qquad \text{(A4)}$$

where $H_0^{(2)}$ is the zero-order Hankel function of the second kind, and

$$r = \sqrt{(x' - x)^2 + (z' - z)^2}$$
$$r_1 = \sqrt{(2X_0 - x' - x)^2 + (z' - z)^2}. \qquad \text{(A5)}$$

This choice makes $\frac{\partial G}{\partial x}\big|_{x = X_0}$ vanish; therefore (A3) becomes

$$\phi(x, z) = -\int_{-\infty}^{\infty} dz'\, G(x - X_0, z - z') \frac{\partial\phi}{\partial x'}\Bigg|_{x' = X_0} \qquad \text{(A6)}$$

where $G(x - X_0, z - z')$ is defined by (16).

ACKNOWLEDGMENT

The authors are indebted to Dr. R. B. Wu and Dr. S. K. Jeng for valuable discussions. Suggestions from the reviewers are also much appreciated.

REFERENCES

[1] P. J. B. Clarricoats and A. B. Sharpe, "Modal matching applied to a discontinuity in a planar surface waveguide," *Electron. Lett.*, vol. 8, pp. 29–29, Jan. 1972.

[2] G. A. Hockham and A. B. Sharpe, "Dielectric-waveguide discontinuities," *Electron. Lett.*, vol. 8, pp. 230–231, May 1972.

[3] G. H. Brooke and M. M. Z. Kharadly, "Step discontinuities on dielectric waveguides," *Electron. Lett.*, vol. 12, pp. 473–475, Sept. 1976.

[4] ____, "Scattering by abrupt discontinuities on planar dielectric waveguides," *IEEE Trans. Microwave Theory Tech.*, vol. MTT-30, pp. 760–770, May 1982.

[5] S. F. Mahmoud and J. C. Beal, "Scattering of surface waves at a dielectric discontinuity on a planar waveguide," *IEEE Trans. Microwave Theory Tech.*, vol. MTT-23, pp. 193–198, Feb. 1975.

[6] T. E. Rozzi, "Rigorous analysis of the step discontinuity in a planar dielectric waveguide," *IEEE Trans. Microwave Theory Tech.*, vol. MTT-26, pp. 738–746, Oct. 1978.

[7] T. E. Rozzi and G. H. In'tVeld, "Field and network analysis of interacting step discontinuities in planar dielectric waveguides," *IEEE Trans. Microwave Theory Tech.*, vol. MTT-27, pp. 303–309, Apr. 1979.

[8] ____, "Variational treatment of the diffraction at the facet of d.h. lasers and of dielectric millimeter wave antennas," *IEEE Trans. Microwave Theory Tech.*, vol. MTT-28, pp. 61–73, Feb. 1980.

[9] T. Hosono, T. Hinata, and A. Inoue, "Numerical analysis of the discontinuities in slab dielectric waveguides," *Radio Sci.*, vol. 17, pp. 75–83, Jan.–Feb. 1982.

[10] C. N. Capsalis, J. G. Fikioris, and N. K. Uzunoglu, "Scattering from an abruptly terminated dielectric-slab waveguide," *J. Lightwave Technol.*, vol. LT-3, pp. 408–415, Apr. 1985.

[11] P. Gelin, S. Toutain, and J. Citerne, "Scattering of surface waves on transverse discontinuities in planar dielectric waveguides," *Radio Sci.*, vol. 16, pp. 1161–165, Nov.–Dec. 1981.

[12] H. Shigesawa and M. Tsuji, "Mode propagation through a step discontinuity in dielectric planar waveguide," *IEEE Trans. Microwave Theory Tech.*, vol. MTT-34, pp. 205–212, Feb. 1986.

[13] K. Morishita, S.-I. Inagaki, and N. Kumagai, "Analysis of discontinuities in dielectric waveguides by means of the least squares boundary residual method," *IEEE Trans. Microwave Theory Tech.*, vol. MTT-27, pp. 310–315, Apr. 1979.

[14] D. Marcuse, "Radiation losses of tapered dielectric slab waveguides," *Bell Syst. Tech. J.*, vol. 49, pp. 273–290, Feb. 1970.

[15] S. Miyanaga and T. Asakura, "Intensity profile of outgoing beams from tapered grating couplers," *Radio Sci.*, vol. 17, pp. 135–143, Jan.–Feb. 1982.

[16] M. Suzuki and M. Koshiba, "Finite element analysis of discontinuity problems in a planar dielectric waveguide," *Radio Sci.*, vol. 17, pp. 85–91, Jan.–Feb. 1982.

[17] S.-J. Chung and C. H. Chen, "Analysis of irregularities in a planar dielectric waveguide," *IEEE Trans. Microwave Theory Tech.*, vol. 36, pp. 1352–1358, Sept. 1988.

[18] S.-J. Chung and C. H. Chen "Partial variational principle for electromagnetic field problems: Theory and applications," *IEEE Trans. Microwave Theory Tech.*, vol. MTT-36, pp. 473–479, Mar. 1988.

[19] O. C. Zienkiewicz, *The Finite Element Method.* New York: McGraw-Hill, 1977.

[20] E. Hinton and D. R. J. Owen, *Finite Element Programming.* New York: Academic Press, 1977.

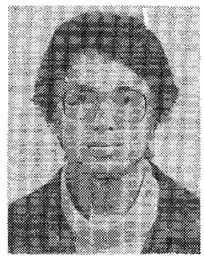

Shyh-Jong Chung was born in Taipei, Taiwan, Republic of China, on January 18, 1962. He received the B.S.E.E. degree in June 1984, and the Ph.D. degree in July 1988, both from National Taiwan University, Taipei, Taiwan. His topics of interest include waveguide discontinuity problems, integrated optics, wave propagation, and numerical techniques in electromagnetics.

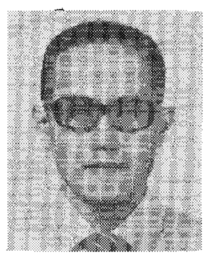

Chun Hsiung Chen was born in Taipei, Taiwan, Republic of China, on March 7, 1937. He received the B.S.E.E. degree from National Taiwan University, Taipei, Taiwan, in 1960, the M.S.E.E. degree from National Chiao Tung University, Hsinchu, Taiwan, in 1962, and the Ph.D. degree in electrical engineering from National Taiwan University in 1972.

In 1963 he joined the faculty of the Department of Electrical Engineering, National Taiwan University, where he is now a Professor. From August 1982 to July 1985 he was Chairman of the department. In 1974 he was a Visiting Researcher for one year at the Department of Electrical Engineering and Computer Sciences, University of California, Berkeley. From August 1986 to July 1987, he was a Visiting Professor at the Department of Electrical Engineering, University of Houston, TX. His areas of interest include antenna and waveguide analysis, propagation and scattering of waves, and numerical techniques in electromagnetics.